

## String models of glueballs and the spectrum of $SU(N)$ gauge theories in 2+1 dimensions

Robert W. Johnson and Michael J. Teper

*Theoretical Physics, University of Oxford, 1 Keble Road,  
Oxford OX1 3NP, UK*

### **Abstract.**

The spectrum of glueballs in 2+1 dimensions is calculated within an extended class of Isgur-Paton flux tube models and compared to lattice calculations of the low-lying  $SU(N \geq 2)$  glueball mass spectrum. Our modifications of the model include a string curvature term and a new way of dealing with the short-distance cut-off. We find that the generic model is remarkably successful at reproducing the positive charge conjugation,  $C = +$ , sector of the spectrum. The only large (and robust) discrepancy involves the  $0^{-+}$  state, raising the interesting possibility that the lattice spin identification is mistaken and that this state is in fact  $4^{-+}$ . Additionally, the Isgur-Paton model does not incorporate any mechanism for splitting  $C = -$  from  $C = +$  (in contrast to the case in 3+1 dimensions), while the ‘observed’ spectrum does show a substantial splitting. We explore several modifications of the model in an attempt to incorporate this physics in a natural way. At the qualitative level we find that this constrains our choice to the picture in which the  $C = \pm$  splitting is driven by mixing with new states built on closed loops of adjoint flux. However a detailed numerical comparison suggests that a model incorporating an additional direct mixing between loops of opposite orientation is likely to work better; and that, in any case, a non-zero curvature term will be required. We also point out that a characteristic of any string model of glueballs is that the  $SU(N \rightarrow \infty)$  mass spectrum will consist of multiple towers of states that are scaled up copies of each other. To test this will require a lattice mass spectrum that extends to somewhat larger masses than currently available.

PACS numbers: 11.15.Kc, 12.38.Gc, 12.39.Mk

# 1 Introduction

While it is now possible to calculate the spectrum of continuum non-Abelian gauge theories with some precision, using standard lattice Monte Carlo techniques [1, 2, 3], we know little about the structure of these glueballs. This is to be contrasted with states containing quarks where, at least for the low-lying spectrum, the quark model provides a remarkably successful semi-quantitative model framework for understanding the structure of mesons and baryons. (Apart from the interesting cases of scalar mesons and pseudoscalar flavour-singlet mesons.)

The glueballs of the  $SU(3)$  non-Abelian gauge theory in 3+1 dimensions are particularly important because the presence of such extra non-quarkonium states in the spectrum of QCD (and in the experimental spectrum) would provide a direct reflection of the gauge fields in the theory. Understanding just how they do so (mixing, decays etc.) would be made easier if we understood something about their structure. Unfortunately, beyond providing some information about glueball sizes, lattice Monte Carlo calculations have as yet given us little insight into their structure. Such calculations involve connected correlators of several operators and while they are simple in principle it is, in practice, much harder to achieve sufficient statistical accuracy than in the corresponding mass calculations.

An alternative way to learn about the structure of glueballs is through a reliable model – just as the quark model provides us with useful information on the structure of the low-lying mesons and baryons. To establish whether a glueball model is ‘reliable’ one can compare the spectrum it predicts to the known spectrum (as calculated from the lattice). This is the approach we follow here. There are two obvious models that one might try: constituent gluon models, such as gluon potential [4] and bag models [5], or flux tube (string) models [6]. In this paper we shall confine ourselves to a study of the latter.

Models try to isolate the essential physics and neglect everything else; thus they necessarily involve approximations. So one does not expect precise agreement with the known spectrum. If we are only looking for semi-quantitative or even qualitative agreement, it is important to test the model in as many relevant contexts as possible. One fact we can usefully use here is that string models (and indeed bag models) can be equally motivated in any gauge theory that has linear confinement and hence string-like flux tubes. This suggests that it would be useful to test this model not only in 3+1 dimensions [7] but also in 2+1 dimensions where non-Abelian gauge theories appear to be linearly confining and detailed mass spectra are available [3]. This is what we shall do in this paper. (We remark that recent improvements in the lattice calculation of the  $D=3+1$   $SU(3)$  spectrum [2] warrant a complete update of the study in [7].)

In the next section we briefly review the Isgur-Paton flux tube model for glueballs [6] and describe the qualitative features of the mass spectrum that it predicts for  $SU(N)$  gauge theories in  $D=2+1$ . We compare this spectrum with the ‘true’ spectrum as calculated on the lattice, [3], which, for the reader’s convenience, we summarise in

Table 1 borrowed from [3]. We point out where the main discrepancies and difficulties lie and we point out some compelling generalisations of the model. In the subsequent section we address a major such difficulty: how to incorporate an acceptable  $C = \pm$  splitting into the model. We finish with a summary of our results. Finally we remark that a summary of some of our preliminary results has appeared elsewhere [9], and a much more detailed exposition appears in [10].

## 2 The Isgur-Paton flux tube model of glueballs

Consider a quark and an antiquark sufficiently far apart. In a linearly confining theory, they will be joined by a flux tube which contributes an energy that is approximately proportional to its length. One can attempt to use such states as the basis for a flux tube model of quarkonia. The corresponding model for glueballs would be based on a loop of fundamental colour flux that closes on itself. This colour singlet object contains no quarks. If we neglect its thickness, we have a closed string of flux, and the glueball mass spectrum is obtained by finding the energy eigenstates of the quantised string. This is the starting point for the Isgur-Paton model [6] and our consequent extensions.

We start with a closed string of colour flux in the form of a circle of radius  $\rho$  with bare string tension  $\sigma_b$ , and hence a bare energy

$$E_b = 2\pi\sigma_b\rho. \quad (1)$$

Fluctuations about this circle are decomposed into discrete phonons of definite helicity. These phonons carry angular momentum, and so there must be a term proportional to the total phonon number  $M$ , given by

$$E_{phonons} \equiv \frac{M}{\rho} = \frac{1}{\rho} \sum_{m=2} m(n_m^+ + n_m^-) \quad (2)$$

added to the total energy of the state. Note that the above sums begin with the  $m = 2$  mode. The  $m = 1$  mode is excluded in the model [6] because infinitesimal  $m = 1$  fluctuations are the same as infinitesimal translations of the circle.

As usual when one quantises over modes of all frequencies there is a divergent contribution to the vacuum energy. Part of this divergent piece can be absorbed into the renormalised string tension,  $\sigma = \sigma_b + c/2\pi$ . The rest appears as a string Casimir energy. It is universal for bosonic strings and, in the case where the strings end on static quarks, is called the Lüscher term [11]. In the present case the string has periodic rather than fixed boundary conditions, just as in calculations involving Polyakov loops [12], but the coefficient differs due to the exclusion of the  $m = 1$  mode. Putting all this together we can write the energy of the string plus its modes as

$$E_s = 2\pi\rho\sigma - \frac{13}{12\rho} + \frac{1}{\rho} \sum_{m=2} m(n_m^+ + n_m^-) \quad (3)$$

However, we know that what we have is not really a one-dimensional string but rather a flux tube whose width will be  $\sim 1/\sqrt{\sigma}$ . For the low-lying states of interest to us we expect  $\rho \sim 1/\sqrt{\sigma}$  and so one might expect the simple harmonic fluctuations of the flux tube to be somehow suppressed. This is incorporated within the Isgur-Paton model [6] by multiplying the contribution of the phonons to the energy (including that of the vacuum) by a heuristic suppression factor that rapidly approaches unity as  $\rho$  increases. This leads to a final string energy

$$E_s^M(\rho) = 2\pi\rho\sigma + \frac{M + \gamma}{\rho}F(\rho) \quad (4)$$

where  $\gamma = -13/12$ ,  $M$  is defined in eqn(2) and  $F(\rho)$  is the factor that suppresses the string excitations at small  $\rho$ . In the original model this was chosen to be  $F(\rho) = 1 - e^{-f\rho}$ , where  $f$  is a parameter which we would expect to be  $O(\sqrt{\sigma})$ . This form is reasonable but somewhat arbitrary; one might ask, for example, why the string energy,  $2\pi\rho\sigma$ , is not modified at small  $\rho$  as well.

To quantize the string, we must take into account its motion in the radial direction as well. In the Isgur-Paton model one identifies the conjugate momentum for the string and writes a Schrodinger equation in the radial coordinate  $\rho$ :

$$\left\{ \frac{-9}{16\pi\sigma} \frac{d^2}{d\xi^2} + E_s^M(\xi^{2/3}) \right\} \psi(\xi) = E\psi(\xi) \quad (5)$$

where  $\xi = \rho^{3/2}$  turns out to be the natural variable to use here. This formalism assumes that the phonon modes are ‘fast’ compared to the collective radial modes and that they can therefore be treated as providing an effective potential for these latter modes. Clearly such an ‘adiabatic’ assumption is at best approximate: the model has only one scale,  $\sqrt{\sigma}$ , and so there is no reason for the phonon fluctuations to be *much* faster than the collective radial fluctuations for the low-lying part of the spectrum that will interest us. (Indeed if one calculates [7] the low-lying spectrum one finds that the energy splitting associated with an increment in the phonon number is of the same order as the splitting associated with an increment in the radial quantum number. This suggests that the division into fast and slow modes is a crude approximation at best.)

If we were in 3+1 rather than in 2+1 dimensions, the above description of the model would change as follows. First, rotations of the flux-loop around a diameter provide an additional source of angular momentum, and equation(5) acquires a corresponding angular momentum term. In addition there are extra phonons arising from fluctuations of the loop normal to its plane. This doubling of modes leads to a doubling of the value of the string Casimir energy in eqn(3).

The simplest version of the Isgur-Paton model sets  $F(\rho) = 1$  in equation(4) so that there is no fudge factor. Since  $\sigma$  merely sets the overall scale of the mass spectrum, the mass ratios  $m/\sqrt{\sigma}$  are then predicted with no free parameters at all. These prediction

(borrowed from reference [7]) are listed in Table 2. The comparison is with  $SU(N \rightarrow \infty)$ , since in that limit, just as in the model, heavy glueballs do not decay. The overall qualitative agreement is remarkable, with only the  $0^{-+}$  far from its prediction in the  $C = +$  sector, and motivates the more detailed investigation of this paper.

### 3 Generalising the Isgur-Paton flux tube model

In this section we point to several ways in which the original Isgur-Paton model can be generalised. We start with the observation that one can build on other strings than the fundamental. We then point out that a curvature term in the effective string action makes an important difference. The argument for both these extensions is compelling. We then turn to the short-distance fudge factor  $F(\rho)$  in eqn(4), point out its shortcomings and suggest some alternatives. We leave to the next section the important question of how to split the  $C = \pm$  spectra in a way that is both natural in terms of the string model and reproduces the main features of the observed splitting.

#### 3.1 Extra strings, extra states

The flux tube in the Isgur-Paton model contains flux in the fundamental representation; it joins charges that are in that representation. For  $SU(N \geq 4)$  there exist charges in higher representations which cannot be screened by virtual adjoint charges (i.e. gluons) down to the fundamental. One can label charges in these representations by the way they transform under a centre gauge transformation,  $z \in Z_N$ . If they acquire a factor  $z^k$  we will refer to them as having  $N$ -ality  $k$ . Since gluons transform trivially under the centre they cannot screen the  $N$ -ality of a charge. For each such charge we have a flux tube of a corresponding  $N$ -ality  $k$ , which will possess a string tension  $\sigma_k$ . We can consider a closed tube of such flux, and we can then build a whole spectrum of glueball states on this flux string just as we did for the fundamental,  $k = 1$ , string in the Isgur-Paton model. Thus as  $N$  grows the spectrum will acquire extra towers of states that are identical to the spectrum obtained with the fundamental flux loop except that their overall energy scale is  $\sqrt{\sigma_k/\sigma_1}$  (ignoring any mixing).

If observed, such a spectrum would be a remarkable manifestation of the underlying string structure of glueballs. Of course it is not guaranteed that such a spectrum actually exists in the string picture: this will depend on the dynamics. Consider for example the case of  $SU(4)$ . If it happens to be the case that  $\sigma_{k=2} \not\approx 2\sigma_{k=1}$  then the  $k = 2$  flux tube can break up into two  $k = 1$  (fundamental) flux loops, so that the  $k = 2$  states are just multi-glueball scattering states formed out of the  $k = 1$  glueball states. In the  $SU(4)$  gauge theory it is known [17] that  $\sigma_{k=2} \simeq 1.4\sigma_{k=1}$  in both  $D=2+1$  and  $D=3+1$ , and so the corresponding extra states should exist there. However the lattice calculations have not identified enough excitations (in each  $J^{PC}$  sector) to test for the possible presence of such extra states, so we will ignore this potential state

replication in the remainder of this paper, apart from pointing to its great interest for future calculations [10].

### 3.2 Curvature/elasticity

The flux tube must have a finite thickness if it is to have a finite energy density; presumably it will be  $O(1/\sqrt{\sigma})$ . Such a finite flux tube will presumably possess an effective elasticity. In string language this is a curvature term. For a meson, the curvature of the straight string joining the quarks is zero and so a curvature term would have no effect to the order in  $1/\rho$  that we are including. For a closed string, on the other hand, the curvature is constant and integrates to a  $\sim 1/\rho$  contribution. The constant of proportionality, our effective elasticity, we denote by  $\gamma_E$  and we will regard it as an unknown free parameter. Note that we may regard the Casimir energy of the closed loop as simply renormalizing the elasticity

$$\gamma = \gamma_E - \frac{13}{12} \quad (6)$$

just as the  $c\rho$  piece was absorbed into a renormalisation of  $\sigma$ . Although there has been some discussion [18] as to the sign such an elasticity should take, we shall leave  $\gamma$  as a free parameter, whose value is to be determined by fitting the spectrum.

### 3.3 Modification at short distances

Since the flux tube has a finite width, a glueball will presumably cease to look like an excited closed string when  $\rho$  is much less than that width. This is embodied in the Isgur-Paton model by a fudge-factor  $F(\rho) = 1 - e^{-f\rho}$  which suppresses the contribution of the string phonons as  $\rho \rightarrow 0$ , as in eqn(4). The detailed form of  $F(\rho)$  is largely arbitrary, as is the choice to suppress the phonon excitations but not the  $2\pi\rho$  string contribution. Since the spectrum of the string model is non-singular when we set  $F(\rho) = 1$ , the effects of the suppression factor are not large and the details do not matter greatly. We have calculated the spectrum for various possibilities and we find that as far as the  $C = +$  spectrum is concerned what one needs is a modest short-distance suppression so as to get the  $0^{++}, 2^{++}$  splitting about right, and then one can tune the  $\gamma/\rho$  contribution so as to raise the overall spectrum to about the right level.

A quite different possibility is to make the string tension a function of  $\rho$  rather than to impose a fudge-factor  $F(\rho)$ . This is motivated by a recent study [19] of closed flux tubes in the dual Ginzburg-Landau theory. They find that the effective string tension,  $\sigma_{eff}(\rho)$ , varies with  $\rho$  so as to vanish as  $\rho \rightarrow 0$ . One can in fact parameterise the observed variation quite accurately using

$$\sigma_{eff}(\rho) = \sigma(1 - e^{-1.72\rho}). \quad (7)$$

One can then quantise the string model with this  $\rho$ -dependent string tension and solve for its spectrum. Since  $\sigma_{eff}(\rho)$  appears in the mass and hence in the kinetic energy of the loop, the quantisation is not entirely straightforward and we leave its description to the Appendix. (More details may be found in [10].) The qualitative effect of using a variable  $\sigma_{eff}(\rho)$  in eqn(5) is that at small  $\rho$  the kinetic energy is enhanced relative to the potential energy. This is much the same as the effect of our fudge-factor  $F(\rho)$ . However it has the advantage that there is no free parameter (or functional form) to choose and there is no ambiguity as to how one should apply it.

## 4 Splitting $C = +$ from $C = -$

For  $N > 2$  the flux tube carries an arrow. In the simple Isgur-Paton model there is no mixing between loops of opposite flux, and the resulting states are degenerate. Since the direction of the flux reverses under charge conjugation  $C$ , this predicts degenerate  $C = \pm$  spectra, as in Table 2. We now turn to the problem of how one might split this  $C = \pm$  degeneracy in a way that is both natural in terms of the string model and reproduces the main features of the observed splitting. We shall begin by summarising what these features are and we shall then consider two possible dynamical mechanisms, direct mixing and adjoint mixing. Additional mechanisms, such as indirect mixing and k-string mixing, are explored in [10]. In each case we shall ask how well the main observed features are reproduced.

### 4.1 The observed $C = +/-$ splitting

From the masses listed in Table 1 we see that the  $C = +/-$  splitting possesses the following qualitative features:

- In Fig.1 we plot two examples of the  $C = \pm$  splitting, as a function of  $1/N^2$ . This is a natural variable to use since the leading corrections to the large- $N$  limit are expected to be  $O(1/N^2)$  [13]. We infer from this plot (and from similar plots of other states) that the splitting remains non-zero in the  $N = \infty$  limit; it is a leading order effect.
- In SU(2) there is no  $C = -$  sector and one can ask what the SU(2)  $0^+$  mass continues to as  $N$  increases. This will clearly depend on the dynamics that produces the  $C = \pm$  splitting for  $N \geq 3$ . For example, if this dynamics simply splits the  $0^{++}$  and  $0^{--}$  equally from their naive degenerate masses, then we would expect the SU(2)  $0^+$  to continue smoothly to the average of the  $0^{++}$  and  $0^{--}$  masses. As another example, if the shift involves just the  $0^{--}$ , then the SU(2)  $0^+$  will continue smoothly to the  $N \geq 3$   $0^{++}$ . Conversely, if the shift affects just the  $0^{++}$ , then the continuation should be with the  $0^{--}$ . In Fig.2 we plot the  $0^{++}$  and  $0^{--}$  masses, as well as the average of the two, as a function of  $1/N^2$ . We see that in all cases the variation with  $N$  for  $N \geq 3$  can be described using just a leading  $\propto 1/N^2$  correction. We also note that the SU(2)  $0^+$  mass extrapolates precisely from the  $0^{++}$  masses while it is inconsistent with a smooth

extrapolation of the averaged  $C = \pm$  states or of the  $0^{--}$ . The same is true for the tensor: the  $SU(2)$   $2^+$  mass is a smooth continuation of the  $SU(N \geq 3)$   $2^{\pm+}$  masses, and not of the average of the  $2^{\pm+}$  and  $2^{\pm-}$  masses, or of the  $2^{--}$ . We shall see that this observation provides a tough constraint on possible mechanisms for splitting the  $C = +$  and  $C = -$  sectors.

- The  $C = \pm$  splitting appears to decrease as the mass increases. To be more specific we infer from

$$m_{0--} - m_{0++} > m_{0--*} - m_{0++*}. \quad (8)$$

that states with larger radial quantum number,  $n_R$ , are split less than those with smaller  $n_R$ . (Recall that in the flux tube model these lowest excitations are radial rather than phonon.) Furthermore we infer from

$$\begin{aligned} m_{0--} - m_{0++} = 1.85(26)\sqrt{\sigma} &> m_{2--} - m_{2++} = 1.01(38)\sqrt{\sigma} \\ &> m_{1--} - m_{1++} = -0.62(65)\sqrt{\sigma} \end{aligned} \quad (9)$$

(obtained at  $N = \infty$ ) that the magnitude of the splitting also decreases with increasing phonon number. (Recall that for the lightest  $J = 0, 2, 1$  glueball states the total phonon number in eqn(2) is  $M = 0, 2, 5$  respectively.) Note that the decrease we see is even faster when the splitting is expressed in terms of the average mass. All this provides constraints on possible splitting mechanisms.

## 4.2 Direct mixing

Since a flux loop has a direction,  $L$  or  $R$ , it is convenient to introduce 2-component wave-functions:

$$\Psi \equiv \begin{pmatrix} \psi_L \\ \psi_R \end{pmatrix}. \quad (10)$$

In this notation, we can write (unnormalized)  $C = \pm$  states as

$$\Psi_{C=+} = \psi \begin{pmatrix} 1 \\ 0 \end{pmatrix} + \psi \begin{pmatrix} 0 \\ 1 \end{pmatrix} \quad ; \quad \Psi_{C=-} = \psi \begin{pmatrix} 1 \\ 0 \end{pmatrix} - \psi \begin{pmatrix} 0 \\ 1 \end{pmatrix} \quad (11)$$

and eqn(5) becomes

$$H_{IP}\Psi = \begin{bmatrix} H_L & 0 \\ 0 & H_R \end{bmatrix} \begin{pmatrix} \psi_L \\ \psi_R \end{pmatrix} = E\Psi \quad (12)$$

where  $H_L \equiv H_R$  is the operator on the LHS of eqn(5).

With the above Hamiltonian there is no mixing between  $L$  and  $R$  states and hence no  $C = \pm$  splitting. To obtain such a splitting we need a non-zero probability for a  $L$  state to turn into an  $R$  state and vice-versa, which clearly requires some off-diagonal terms to appear in the Hamiltonian  $H$ . So we alter eqn(12) to define our ‘direct mixing’ Hamiltonian as

$$H_{dir}\Psi = \begin{bmatrix} H_L & \alpha \\ \alpha & H_R \end{bmatrix} \begin{pmatrix} \psi_L \\ \psi_R \end{pmatrix} = E\Psi \quad (13)$$

where we shall choose to keep  $\alpha$  real and constant. A simple motivation for such a mixing arises from the observation that when the radius of the flux loop is less than the flux tube width, we have something that is no longer a distinct loop, but is rather some kind of “ball” which will no longer have any definite orientation. In a path integral picture, we can think of a path where a loop of orientation  $L$  (for example) shrinks into a ball, at which point it loses any memory of its initial orientation, and then expands back out into a loop of either orientation with equal probability. This transition will lead to a finite amplitude between  $L$  and  $R$  loops.

We shall return later to ask how well this model fits the spectrum. For now we concentrate on its qualitative predictions, taking the approximation  $H_L = H_R = M$  where  $M$  is the mass of the unmixed state. Then the energy eigenstates are clearly

$$M_{C=\pm} = M \pm \alpha \tag{14}$$

so that  $C = \pm$  states are split equally from their common Isgur-Paton value. Three immediate observations follow from the above:

- For states of approximately equal  $\rho$ , the splitting should be roughly the same independent of the phonon number. This would be the case, for example, for the lightest  $J = 0, 1, 2$  states. However, as we have seen in eqn(9), the splitting does in fact vary a great deal amongst these states.
- It is the average of the  $C = +$  and  $C = -$  masses that equals the mass with no mixing. As we decrease  $N$  from  $N = \infty$  it is this average that should extrapolate to the  $SU(N = 2)$  value of the  $0^+$  mass, because the Hamiltonian there is the same as  $H_L$  or  $H_R$ . (All this up to  $O(1/N^2)$  corrections.) However we have seen in Section 4.1 that this is not the case: the  $SU(2)$   $0^+$  mass equals the  $SU(N \geq 3)$   $0^{++}$  mass up to  $O(1/N^2)$  corrections.
- We expect the wavefunction to have a smooth limit as  $N \rightarrow \infty$ , and so the probability for  $\rho$  to be less than the flux tube radius should also have a non-zero limit. Thus the  $L \leftrightarrow R$  mixing and the consequent  $C = \pm$  splitting should be non-zero at  $N = \infty$ , just as is observed. (This appears to contradict the conventional statement [13] that mixings vanish as  $N \rightarrow \infty$  but we believe that the standard arguments do not apply to our kind of ‘mixing’.)

We might suppose that the first observation becomes irrelevant when we perform the actual numerical calculations, but unfortunately it remains an issue. Moreover, however we tune the parameters in this model, it remains the case that it is the average of the  $0^{++}$  and  $0^{--}$  masses that is predicted to continue smoothly to the  $SU(2)$   $0^+$  mass, and, as we have seen, this is contradicted by the lattice calculations. Thus other, perhaps less straightforward mechanisms need to be considered.

### 4.3 Adjoint string mixing

We pointed out in Section 3.1 that in  $SU(N \geq 4)$  theories there exist extra stable strings and hence extra states. Since these are just scaled up versions of our fundamental

string spectrum they would not help in splitting  $C = +$  from  $C = -$ . However there is another type of string in the theory that we have not yet considered: the one that carries adjoint flux. Such a string carries no arrow: it is intrinsically  $C = +$ . So any mixing would affect the  $C = +$  spectrum: the  $0^{++}$  mass would (probably) be driven down while the  $0^{--}$  would be left undisturbed. But this does not lead to problems with the  $0^+$  in  $SU(2)$  because the same adjoint string exists in  $SU(2)$  and would drive down the  $0^+$  mass there as well. So we have a mechanism that might at last explain why the  $SU(2)$   $0^+$  smoothly interpolates onto the  $0^{++}$  for  $SU(N > 2)$ .

The problem with this mechanism is, of course, that the adjoint string can be broken by gluon pair production so it is not clear if it makes sense to use a closed adjoint loop as the basis for a set of states. However we know that as  $N \rightarrow \infty$  the string becomes stable [13] so at least for large  $N$  it can be used in this way. Since, as we have seen, lattice studies [3] find that the low-lying  $SU(2)$  spectrum differs only by small corrections from  $SU(N = \infty)$ , it is reasonable to assume that the adjoint string has developed only a modest decay width in  $SU(2)$ . (As indeed seems to be the case [23] in 3+1 dimensions.) If so then the decay time will be long compared to the characteristic time scale of the low-lying string modes, and we can safely quantise the string in the Isgur-Paton fashion. We will assume that this is so from now on, although an explicit lattice verification would clearly be very helpful.

We can use an extension of the formalism in the previous subsection to derive the Hamiltonian, defining the wave-function as

$$\Psi = \begin{pmatrix} \psi_+ \\ \psi_- \\ \psi_a \end{pmatrix}. \quad (15)$$

However since  $\psi_a$  always has  $C = +$ , the Hamiltonian

$$H_{adj} = \begin{bmatrix} H_+ & 0 & \alpha_a \\ 0 & H_- & 0 \\ \alpha_a & 0 & H_a \end{bmatrix} \quad (16)$$

is quite simple: we can clearly reduce it to a two-component calculation in the  $C = +$  sector, and a simple Isgur-Paton calculation in the  $C = -$  sector. We shall assume that there is no mixing between fundamental and adjoint loop states that have differing phonon occupation numbers.

In eqn(16)  $H_+ = H_-$  is the usual Isgur-Paton Hamiltonian.  $H_a$  will be identical except that the scale is set by the adjoint string tension,  $\sigma_a$ , rather than by the fundamental  $\sigma$ . It is frequently speculated that  $\sigma_a$  and  $\sigma$  are related by the ratio of quadratic Casimirs

$$\frac{\sigma_a}{\sigma} = \frac{2N^2}{N^2 - 1}. \quad (17)$$

Lattice calculations in  $D = 2 + 1$  [22] find that for  $SU(2)$   $\sigma_a \simeq 2.5\sigma$ , which is quite close to the value of  $8/3$  one obtains from eqn(17). Thus we expect states based on the

adjoint loop to be about a factor of  $\sqrt{2.5} \sim 1.5$  heavier than corresponding states based on the fundamental loop, and so quite massive. Indeed, if we assume a simple two body mixing, with  $H_+$  replaced by  $M = m_{0--}$  and  $H_a$  by  $M_a \simeq 1.5M$ , and if we choose  $\alpha$  so as to obtain the observed  $m_{0++}$  mass, we find that the lightest scalar ‘adjoint’ state has  $M_{a,0++} \simeq 1.8m_{0--}$ . This is light enough to be important by its explicit presence in the spectrum, in addition to affecting the fundamental states through mixing.

How can the fundamental flux loop mix with an adjoint loop? Once again our underlying physical picture is that, for small  $\rho$ , these loops of string become rather like ‘balls’ of flux instead, which may reemerge as a loop of different orientation, or indeed even of a different type of flux. We now have the following qualitative predictions:

- As with the direct mixing of Section 4.2, we expect the mixing, and hence the splitting, to be leading order in  $N$ , as is observed.
- As remarked above, since the adjoint loop mixes with just the  $C = +$  sector and does so for all  $SU(N \geq 2)$  gauge theories, we expect the  $SU(2)$   $0^+$  mass to continue smoothly on to the  $SU(N > 2)$   $0^{++}$  masses, as is observed.
- Whether the splitting decreases with increasing phonon number  $M$  at fixed radial number  $n_R$  is however not clear – it requires a detailed calculation.

The observed pattern of the  $C = \pm$  splitting has proved very constraining on possible dynamics, but the model in which the fundamental loop mixes with an adjoint loop appears to have the right qualitative features. In the next section we shall see how well it can do at the quantitative level.

## 5 Fitting the lattice spectrum

We have performed a large variety of comparisons with the lattice spectrum. We have used the different  $C = \pm$  splitting mechanisms described in this paper; we have fitted to all the lattice masses or just to a more reliable subset as discussed above; we have used the actual errors in the  $\chi^2$  or expanded errors as described below; we have used explicit short distance fudge factors of various kinds or a  $\rho$ -dependent string tension as described earlier, or indeed no suppression at all. The reader will be relieved to learn that we do not intend to describe this very large number of model fits here but will rather focus on two of the most relevant examples. Some different model fits can be found in [9] and others will appear in [10].

The generalised flux tube model typically has two or three unknown parameters. First there is  $\gamma$ , the (renormalised) curvature/elasticity. Secondly there is the mixing parameter characterised by a strength  $\alpha_0$ . There is the parameter  $f$  which characterises the short-distance cut-off imposed in the Isgur-Paton model. Alternatively we can use  $\sigma_{eff}(\rho)$  instead of  $\sigma$  at short distances and this enables us to do without the parameter  $f$ . We can then solve the model for various values of these parameters and find which fits the lattice spectrum the best.

In this section we will describe what we find when we fit the lattice data with

adjoint string mixing, as described in Section 4.3, or with direct mixing, as described in Section 4.2. In both cases we shall use a  $\rho$ -dependent string tension, as described in Section 3.3, to embody the short distance corrections to the flux tube picture, in a way that introduces no new parameters. In our physical picture of the mixing, we see it as occurring at small  $\rho$  and so we choose the mixing term in eqns(13, 16) to satisfy

$$\alpha(\rho) = \alpha \left( 1 - \frac{\sigma_{eff}(\rho)}{\sigma_{eff}(\infty)} \right) \quad (18)$$

(where we now drop the subscript on  $\alpha_a$ ). In the case of adjoint mixing we determine the adjoint string tension from eqn(17). Thus there are two parameters to be fitted:  $\gamma = \gamma_E - 13/12$ , where  $\gamma_E$  is the string curvature described in Section 3.2, and  $\alpha$ , the mixing strength.

There are however some problems with just taking the mass spectrum as given in Table 1 and doing a least- $\chi^2$  fit on the model parameters. First we have already seen that the model prediction is going to be far from the lattice  $0^{-+}$ , so including it in the fit might badly distort the final ‘best fit’. Moreover there are theoretical reasons for thinking that the lattice  $0^{-+}$  spin assignment might be mistaken and that this is actually a  $4^{-+}$ . (And, similarly, that the lattice  $0^{+-}$  is really a  $4^{+-}$ .) To a lesser extent similar questions arise with the purported  $J = 1$  states. We shall therefore exclude these states from the fit but will instead quote the values for these masses, as predicted by the best fit to the other states.

A second problem is that the most accurate masses are for the lightest states. Having the smallest errors these will provide the most important component of the  $\chi^2$  function that determines the best fit. On the other hand the lightest states possess the smallest radius  $\rho$  and so we expect the flux loop model to suffer the largest corrections for such states. Thus we might not want them to dominate, and so possibly distort, the best fit.

This second problem has no unambiguous resolution. The fact is that we know that the model is a simple approximation that can at best incorporate only the essential features of glueball structure. The most that we can expect is that it roughly reproduces the spectrum and whether it can do so is what we want to learn when we fit the model to the data. To do this we need to embody what we mean by ‘roughly’ in some specific way into the fitting procedure. In order not to be unduly biased by the very small errors on the lightest masses, we have enhanced all the errors by 5% of the mass, and add it in quadrature with the statistical error. In practice the best fits turn out to be similar whether we perform such an enhancement or not. That is to say, we are saying that we want to know if the model can fit the masses within  $\pm 5\%$ . Of course the best fit might do better than that; but at least it will not be driven by the very small errors on the lightest masses for which it is probably least reliable.

In each case we obtain the predicted spectrum by solving the coupled set of differential equations, using the numerical technique detailed in [10], on a grid in parameter

space, and then we perform a final simplex minimization starting at the most favorable grid point to find the best  $\chi^2$  fit. (With just two parameters such a crude approach works reasonably well.) The best fit is determined using the lightest three states in the  $0^{++}$  and  $0^{--}$  sectors, and the two lightest states in the  $2^{\pm+}$  and  $2^{\pm-}$  sectors.

We have remarked that there are reasons to think that these simple models should work best in the  $N \rightarrow \infty$  limit, and so we display the results of fitting to the lattice spectrum as extrapolated to  $N \rightarrow \infty$ . A more thorough display of the results for all  $N$  may be found in [10]. In Table 4 we show the mass spectra for the adjoint mixing mechanism, and in Table 3 we present the values of the fitted parameters, for all values of  $N$ . In Figure 3 we display the spectrum at  $N = \infty$ . The corresponding spectra for the direct mixing mechanism are shown in Table 6, and in Table 5 are the parameters for the direct mechanism. Figure 4 displays the direct mixing spectrum at  $N = \infty$ .

We see from the Figures that the best fits, whether obtained using the direct or the adjoint mixing mechanisms, are of an overall reasonable quality. A closer examination of the detailed spectra does however show that both models have some minor difficulties. The direct mechanism has problems with the excitations in the  $J=0$  sector: by the time the third excitation is reached, which has a greater average  $\rho$  than the ground state, the conjugate mixing drives the two model states much farther apart than they ought to be. The way that the adjoint mixing model avoids this problem is that the mass of the lightest adjoint loop state is naturally close to that of the  $0^{+++}$ , because  $\sqrt{\sigma_a/\sigma_f} \sim 1.5$ . Thus, after mixing, the  $0^{+++}$  can be largely an adjoint loop, and the  $0^{++}$  can then be (largely) the first fundamental loop excitation. However, the direct mixing mechanism does have numerically better values of  $\chi^2$ , and thus we ought to consider it more likely than the adjoint mixing mechanism. This suggests that a flux tube model that combines both direct and adjoint mixing should be able to do much better than either model alone. Combining these models is quite natural; our picture for the way an oriented fundamental loop may evolve into an adjoint loop (through contracting into a small ‘disoriented’ ball) is precisely the way we saw the direct mixing between fundamental loops of opposite orientation proceeding. This picture will, in general, require two mixing parameters. While it is interesting to explore these ideas [10] the analysis would clearly benefit from improved lattice calculations where a larger number of excited states are accurately determined.

Returning to the best fit parameters listed in Tables 3 and 5, we observe that all our fits require  $\gamma$  to be positive or very close to zero. Ignoring the values for  $SU(2)$ , there is a trend in the values of  $\gamma$  consistent with a  $\frac{1}{N^2}$  relationship; see [10] for more details. Taken together with eqn(6) this tells us that the observed mass spectra do indeed require a non-zero curvature (elasticity) term,  $\gamma_E \in [0.5, 1.0]$ , in the effective string model for the confining flux tube.

From either Figure 3 or Figure 4 we see that the conventional spin assignments of the heavier states are called into question. The model consistently puts the  $4^{-+}$  and the  $4^{+-}$  states at masses corresponding to lattice states with spin 0. These states do

not contribute to the  $\chi^2$ , and so their masses are purely predictive—the agreement is remarkable. Furthermore, while the lattice states  $1^{\pm+}$  agree with the model’s predictions for the lightest state with  $M = 5$  (which is the smallest value of  $M$  giving spin 1), the states conventionally labelled  $1^{\pm-}$  are at the mass predicted for states with  $M = 3$ . These states are also related by a spin ambiguity of *modulo*4 on a cubic lattice, and so we must also investigate these assignments in the future as well.

Finally we remark that the features we have described are not only robust against the detailed fitting procedures used but much the same conclusions are obtained if we replace the  $\rho$  dependence of the string tension with a short distance modification of the kind shown in eqn(4).

## 6 Conclusions

In this paper we set out to test the idea that glueballs are quantised closed strings of colour-electric flux. Such a picture arises naturally in linearly confining theories, such as  $SU(N)$  gauge theories in 2+1 and 3+1 dimensions, where distant fundamental charges are connected by flux tubes.

We started out with the specific dynamical framework of the Isgur-Paton flux tube model [6], in which the excitations of the closed flux loop are either radial or phonon-like, and we confronted its mass spectrum with the rather accurate mass spectra available in D=2+1  $SU(N)$  gauge theories [3]. As  $N \rightarrow \infty$  the gauge theory simplifies in ways which bring it closer to some of the model’s assumptions, e.g. the neglect of decays, and so one can argue that a comparison in this limit makes particular sense. If we express the observed masses in units of the observed string tension, then the model’s predictions for these dimensionless ratios involve no free parameters at all. We found that these predictions were, for the most part, quite remarkably good in the  $C = +$  sector of states; and for the  $C = -$  sector they embodied the main qualitative features even if the quantitative comparison was less good.

Of course, when the flux tube radius,  $\rho$ , is smaller than the flux tube width the picture must break down, embodied in the model by suppressing the potential energy below  $\rho \sim 1/f$ , where  $f$  is a parameter that needs to be determined but which we expect to be  $O(\sqrt{\sigma})$ . In this paper we described other ways of including such a cut-off; in particular through a dependence of the string tension on  $\rho$ . By taking  $\sigma(\rho)$  from calculations in the literature [19], one can avoid having the additional parameter  $f$  to fit. We then pointed out that one should in general include a string curvature term, which for a closed loop will make a contribution  $\gamma_E/\rho$  to the effective potential that is of the same form as the Casimir string energy. This introduces a parameter  $\gamma$  that needs to be determined. Finally we noted that the  $C = \pm$  degeneracy in the model mass spectrum is contradicted by the splittings seen in the lattice spectrum and we were compelled to consider dynamical mechanisms that might reproduce these splittings. Such mechanisms typically involve a mixing parameter  $\alpha$  that also needs

to be determined. In searching for the best fit to the observed spectrum, we found that whatever mixing mechanism we used we invariably required a substantial positive string curvature contribution,  $\gamma_E \in [0.5, 1]$ .

The qualitative features of the observed  $C = \pm$  splittings proved to be very constraining. The only mechanism that we were able to construct that was natural, simple and had the right qualitative behaviour, involved adding to the basic flux tube model a sector of states built on closed loops of adjoint flux. These are intrinsically  $C = +$  and we introduced a mixing between these states and the  $C = +$  states built on the fundamental loop. We pictured the mixing as arising at small  $\rho$  where a closed flux tube becomes a flux-less ‘ball’, and we conjectured that this kind of mixing may be leading order in  $1/N$ , as required by the lattice spectrum. The implication of these calculations and also calculations with other mixing mechanisms, such as a direct mixing between fundamental loops of opposite orientation, was that the simultaneous presence of adjoint loop and direct mixing was likely to be much more successful in quantitatively reproducing the observed spectrum.

However even these best fits always left us with one very large discrepancy: the  $0^{-+}$  state. In the model this is a highly excited state (involving eight phonon units) and is predicted to be much heavier than the lattice  $0^{-+}$ . This is a robust result of the model: the splitting of the  $0^{++}$  and  $2^{++}$  states, which is two phonon units, is what essentially determines the  $0^{-+}$  mass. On the other hand the predicted  $4^{-+}$  mass is very close to the lattice  $0^{-+}$  mass (and also for the model’s  $4^{+-}$  and lattice  $0^{+-}$ ). This suggests that the lattice calculation may have mislabelled this state; after all one cannot distinguish  $J = 0$  from  $J = 4$  by the rotational symmetries of a square lattice. This has provoked lattice calculations that are attempting to resolve this rather basic question [14, 15]. (For a detailed exposition of the problem, as well as a means for its solution, see [10].)

If there are states built on the adjoint loop they will be about half as heavy again as the corresponding states built on the fundamental loop and so only the very lightest are likely to be present in the currently available lattice spectrum. Moreover, since the adjoint loop can break, these states may have large decay widths, their masses may be shifted from their naive values, and perhaps only the lightest states will actually exist. However, with a modest improvement in the quality of the lattice calculations, one could search for their presence. The same improvement would allow us to search for degeneracies between states of differing  $J$  but with the same number of phonon ‘units’. For example there will be an excited  $0^{++}$  with phonon content  $n_{m=2}^+ = n_{m=2}^- = 1$  that should be degenerate with a  $4^{++}$  with phonon content  $n_{m=2}^+ = 2, n_{m=2}^- = 0$ . Such (near) degeneracies provide a characteristic pattern that would test the general dynamics of the Isgur-Paton flux tube model.

In  $SU(N \geq 4)$  gauge theories there are additional strings than the fundamental which will be stable if their string tensions are low enough. In  $D=3+1$  this is expected to be the case on theoretical grounds [16], and indeed is known to be the case for  $SU(4)$  [17, 24]. Thus the string model predicts that, if we neglect mixings and decays, the

observed mass spectrum will contain towers of states that are exact scaled-up replicas of the spectrum arising from the fundamental string, and that the number of these ‘towers’ of states will grow as  $N \rightarrow \infty$ . This is a dramatic and robust prediction of the basic flux tube picture which can and needs to be investigated by lattice calculations.

We have seen that the kind of exercise undertaken in this paper, testing a model against lattice calculations, has a fruitful impact in both directions. We have been forced to generalise the model in ways that, in retrospect, are entirely natural. And the model points to both potential weaknesses in the lattice calculations and motivates specific further calculations that promise to be very informative however they turn out.

## Acknowledgments

We are grateful to Jack Paton for valuable discussions during the course of this work. One of us (RWJ) would like to thank the Rhodes Trust for financial support.

# Appendix

In this Appendix we briefly describe how we derive the canonical variables for the Isgur-Paton model. First we discuss the traditional model's equation, and then we describe how we generalise the formalism to accommodate an effective string tension that varies with the loop radius.

## 1. The Isgur-Paton Hamiltonian

We have a circular loop of mass  $\mu = 2\pi\rho$  which moves in an effective potential provided by the phonon modes etc. as discussed earlier in this paper. Thus the kinetic and potential terms are:

$$T = \frac{p_\rho^2}{4\pi\sigma\rho} \quad ; \quad V = 2\pi\sigma\rho + F(\rho)\frac{M + \gamma}{\rho}. \quad (19)$$

where  $F(\rho)$  is the usual short distance fudge-factor, which we shall now set to unity for convenience. Under the transcription  $p_\rho \rightarrow i\hbar\frac{\partial}{\partial\rho}$  we have (with  $\hbar = 1$ )

$$T = \frac{p_\rho^2}{2\mu} \rightarrow \frac{-1}{4\pi\sigma} \frac{\partial}{\partial\rho} \frac{\partial}{\partial\rho}. \quad (20)$$

We want canonical variables  $\xi, P_\xi$  such that  $T$  is quadratic in  $P_\xi$ . In passing from the above classical system to the quantum system there is an ambiguity how to order the various terms in  $T$ . We choose  $P_\rho = \frac{\partial}{\rho^{\frac{1}{2}}}$  so that  $T \propto P_\rho^2$ . That is to say we choose

$$\xi = \rho^{\frac{3}{2}}, \quad (21)$$

so that

$$T \rightarrow \frac{-1}{4\pi\sigma} \left(\frac{3}{2}\right)^2 \frac{\partial^2}{\partial\xi^2} = \frac{-9}{16\pi\sigma} \frac{\partial^2}{\partial\xi^2} \quad (22)$$

and we arrive at eqn(5).

## 2. Generalising to $\sigma(\rho)$

If the vacuum of non-Abelian gauge theories is a (type-II) dual superconductor, then flux tubes will arise through a dual Meissner effect. Thus it is interesting and relevant to ask how closed flux tubes behave as the radius is varied in the Ginzburg-Landau theory of type-II superconductors. As pointed out in [19] what happens is that the effective string tension  $\sigma_{\text{eff}}(\rho)$  vanishes as  $\rho \rightarrow 0$ , roughly as in eqn(7). If we replace  $\sigma$  in the Isgur-Paton model by such a  $\sigma_{\text{eff}}(\rho)$  we will be providing the model with a short-distance cut-off that is both natural and employs no free parameters. The price

for this is some complication in the quantisation of the model. However, as we shall now see, this is a problem that can be overcome.

As we saw earlier, the tricky term in quantizing the Isgur-Paton model is the kinetic energy, so that is where we will begin. Abusing notation slightly,

$$T = \frac{p_\rho^2}{2\mu} \rightarrow \frac{-1}{4\pi} \left( \frac{\frac{\partial}{\partial \rho}}{\sqrt{\sigma_{\text{eff}}(\rho)\rho}} \right)^2, \quad (23)$$

where  $\sigma_{\text{eff}}(\rho)$  is now included in the  $\rho$  dependence of the kinetic energy. If  $\sigma_{\text{eff}}$  were a constant, we would get  $T$  as in eqn(22). Now we must find a canonical variable  $\xi$  such that

$$\frac{\frac{d\xi}{d\rho} \frac{d}{d\xi}}{\sqrt{\sigma_{\text{eff}}(\rho)\rho}} = \frac{d}{d\xi} \quad (24)$$

or

$$d\xi = \sigma_{\text{eff}}^{\frac{1}{2}}(\rho)\rho^{\frac{1}{2}}d\rho \quad (25)$$

Substituting the function in eqn(7) for  $\sigma_{\text{eff}}$ , we find

$$\xi = \sigma^{\frac{1}{2}} \int d\rho \rho^{\frac{1}{2}} (1 - e^{-1.72\rho})^{\frac{1}{2}}. \quad (26)$$

where the integration constant has been determined by the boundary condition  $\xi(0) = 0$ . This integral cannot be put into closed form, yet we need the inverse function explicitly so as to substitute it into the potential  $V(\rho(\xi))$ . While it would be nice to include explicitly the function from [19], any function which approximates it reasonably well will suffice. So rather than using eqn(7) we shall use a less natural form, but one that will suit our manipulations better. Now, we need a function for  $\sigma_{\text{eff}}(\rho)$  which goes to zero as  $\rho \rightarrow 0$  and which approaches  $\sigma$  as  $\rho \rightarrow \infty$ , and which is integrable with respect to the measure  $\rho^{\frac{1}{2}}d\rho$ . As an example consider

$$\sigma_{\text{eff}}(\rho) = \sigma \left( 1 - e^{-f\rho^{\frac{3}{2}}} \right)^2 \quad (27)$$

which, with a suitable value for  $f$ , will crudely approximate the dependence found in [19]. Performing the integral, and imposing  $\xi(0) = 0$ , we have

$$\xi = \sigma^{\frac{1}{2}} \int d\rho \rho^{\frac{1}{2}} (1 - e^{-f\rho^{\frac{3}{2}}}) = \frac{2}{3}\sigma^{\frac{1}{2}} \left( \rho^{\frac{3}{2}} - \frac{1}{f} + \frac{1}{f}e^{-f\rho^{\frac{3}{2}}} \right). \quad (28)$$

We cannot find the functional inverse explicitly, but as we are ultimately working with a discrete set  $\{\xi_j\}$  related to  $\{t_j\}$ , we can simply solve the equation numerically to give  $\rho_j$  which we can put into the potential  $V = V(\rho(\xi_j))$ . (In practice we have used

$\sigma_{\text{eff}} = \sigma(1 - e^{-f\rho})^2$  which leads to a slightly more complex relation than the above.)  
Returning to the kinetic energy,

$$T \rightarrow \frac{-1}{4\pi} \frac{\partial^2}{\partial \xi^2}, \quad (29)$$

and we proceed with the numerical solution of the discretised equation as described earlier.

## References

- [1] M. Teper, hep-th/9812187.
- [2] C. Morningstar and M. Peardon, Phys. Rev. D60 (1999) 034509 (hep-lat/9901004).
- [3] M. Teper, Phys. Rev. D59 (1999) 014512 (hep-lat/9804008).
- [4] Szczepaniak et. al., Phys. Rev. Lett. 76 (1996) 2011 (hep-ph/9511422).
- [5] G. Karl and J. Paton, Phys. Rev. D61 (2000) 074002 (hep-ph/9910413).  
T. H. Hansson, in *Non-perturbative Methods* (Ed. S.Narison, World Scientific 1985).
- [6] N. Isgur and J. Paton, Phys. Rev. D31 (1985) 2910.
- [7] T. Moretto and M. Teper, hep-lat/9312035.  
T. Moretto, D.Phil Thesis, Oxford University (1993).
- [8] V. Agostini, G. Carlino, M. Caselle, and M.Hasenbusch, Nuc. Phys. B484 (1997) 331 (hep-lat/9607029).
- [9] R. Johnson and M. Teper, Nucl. Phys. Proc. Suppl. 63 (1998) 197 (hep-lat/9709083).
- [10] R. Johnson, DPhil Thesis (<http://www-astro.physics.ox.ac.uk/~rjohnson/thesis.ps>).  
R. Johnson and M. Teper, hep-ph/0012287 v1.
- [11] M. Lüscher, K. Symanzik and P. Weisz, Nucl. Phys. B173 (1980) 365.
- [12] Ph. de Forcrand, G. Schierholz, H.Schneider and M. Teper, Phys. Lett. 160B (1985) 137.
- [13] G. 't Hooft, Nucl. Phys. B72 (1974) 461.  
E. Witten, Nucl. Phys. B160 (1979) 57.  
S. Coleman, 1979 Erice Lectures.  
A. Manohar, 1997 Les Houches Lectures, hep-ph/9802419.
- [14] R. Johnson and M. Teper, Nucl. Phys. Proc. Suppl. 73 (1999) 267 (hep-lat/9808012).
- [15] R. Johnson and M. Teper, in progress.
- [16] A. Hanany, M. Strassler and A. Zaffaroni, Nucl. Phys. B513 (1998) 87 (hep-th/9707244).  
M. Strassler, Nucl. Phys. Proc. Suppl. 73 (1999) 120 (hep-lat/9810059).

- [17] B. Lucini and M. Teper, hep-lat/0012025; hep-lat/0107007.
- [18] H. Kleinert and A. M. Chervyakov, hep-th/9601030.
- [19] Y. Koma, H. Suganuma and H. Toki, Phys. Rev. D60 (1999) 074024 (hep-ph/9902441).
- [20] J. Paton, private communication.
- [21] A. Momen and C. Rosenzweig, Phys. Rev. D56 (1997) 1437.
- [22] G. Poulis and H. Trottier, Phys. Lett. B400 (1997) 358 (hep-lat/9504015).  
P. Stephenson, Nucl. Phys. B550 (1999) 427 (hep-lat/9902002).
- [23] S. Deldar, Phys. Rev. D62 (2000) 034509 (hep-lat/9911008).  
G. Bali, hep-lat/0006022.
- [24] M. Wingate and S. Ohta, hep-lat/0006016.

$m_G/\sqrt{\sigma}$					
state	SU(2)	SU(3)	SU(4)	SU(5)	SU( $\infty$ )
0 <sup>++</sup>	4.718(43)	4.329(41)	4.236(50)	4.184(55)	4.065(55)
0 <sup>++*</sup>	6.83(10)	6.52(9)	6.38(13)	6.20(13)	6.18(13)
0 <sup>+++</sup>	8.15(15)	8.23(17)	8.05(22)	7.85(22)	7.99(22)
0 <sup>--</sup>		6.48(9)	6.271(95)	6.03(18)	5.91(25)
0 <sup>--*</sup>		8.15(16)	7.86(20)	7.87(25)	7.63(37)
0 <sup>---*</sup>		9.81(26)	9.21(30)	9.51(41)	8.96(65)
0 <sup>-+</sup>	9.95(32)	9.30(25)	9.31(28)	9.19(29)	9.02(30)
0 <sup>+−</sup>		10.52(28)	10.35(50)	9.43(75)	9.47(116)
2 <sup>++</sup>	7.82(14)	7.13(12)	7.15(13)	7.19(20)	6.88(16)
2 <sup>+++</sup>		–	8.51(20)	8.59(18)	–
2 <sup>-+</sup>	7.86(14)	7.36(11)	6.86(18)	7.18(16)	6.89(21)
2 <sup>-+*</sup>		8.80(20)	8.75(28)	8.67(24)	8.62(38)
2 <sup>--</sup>		8.75(17)	8.22(32)	8.24(21)	7.89(35)
2 <sup>---*</sup>		10.31(27)	9.91(41)	9.79(45)	9.46(66)
2 <sup>+−</sup>		8.38(21)	8.33(25)	8.02(40)	8.04(50)
2 <sup>+−*</sup>		10.51(30)	10.64(60)	9.97(55)	9.97(91)
1 <sup>++</sup>	10.42(34)	10.22(24)	9.91(36)	10.26(50)	9.98(25)
1 <sup>-+</sup>	11.13(42)	10.19(27)	10.85(55)	10.28(34)	10.06(40)
1 <sup>--</sup>		9.86(23)	9.50(35)	9.65(40)	9.36(60)
1 <sup>+−</sup>		10.41(36)	9.70(45)	9.93(44)	9.43(75)

Table 1: Glueball masses in units of the string tension; in the continuum limit [3]. The SU( $\infty$ ) values are obtained by extrapolating the SU( $N \leq 5$ ) values with an  $O(1/N^2)$  correction.

$m_G/\sqrt{\sigma}$		
$J^{PC}$	SU( $\infty$ )	IP model
$0^{++}$	4.065(55)	3.12
$0^{++*}$	6.18(13)	6.46
$0^{+++}$	7.99(22)	8.72
$2^{\pm+}$	6.88(16)	6.79
$2^{\pm+*}$	8.62(38)	9.06
$0^{-+}$	9.02(30)	13.86
$4^{\pm+}$	–	9.64
$1^{\pm+}$	10.00(25)	10.84
$3^{\pm+}$	–	8.30
$0^{--}$	5.91(25)	3.12
$0^{--*}$	7.63(37)	6.46
$0^{---}$	8.96(65)	8.72
$2^{\pm-}$	7.94(35)	6.79
$2^{\pm-*}$	9.62(66)	9.06
$0^{+-}$	9.47(116)	13.86
$4^{\pm-}$	–	9.64
$1^{\pm-}$	9.38(60)	10.84
$3^{\pm-}$	–	8.30

Table 2: Glueball masses in units of the string tension. Predictions of the simple no-parameter Isgur-Paton flux tube model compared to the actual spectrum of the SU( $N = \infty$ ) theory.

adjoint loop mixing			
group	$\alpha$	$\gamma$	$\chi^2_5/\text{d.o.f}$
SU(2)	$0.86\pm 0.65$	$-0.19\pm 0.07$	0.47
SU(3)	$4.5\pm 0.60$	$0.57\pm 0.09$	1.1
SU(4)	$4.2\pm 0.66$	$0.42\pm 0.08$	1.2
SU(5)	$3.8\pm 0.84$	$0.25\pm 0.08$	1.4
SU( $\infty$ )	$3.3\pm 0.8$	$0.07\pm 0.07$	0.99

Table 3: Best fit parameters of the adjoint mixing model.

state	$m_G/\sqrt{\sigma}$				
	SU(2)	SU(3)	SU(4)	SU(5)	SU( $\infty$ )
$0^{++}$	4.87	4.29	4.09	4.04	3.94
$0^{++*}$	6.84	7.03	6.86	6.86	6.78
$0^{+++}$	8.05	9.05	8.88	8.81	8.51
$0^{--}$		6.04	5.83	5.60	5.36
$0^{--*}$		8.86	8.70	8.53	8.35
$0^{---}$		10.90	10.77	10.63	10.48
$0^{-+}$	14.06	14.13	14.00	13.93	13.78
$0^{+-}$		14.21	14.07	13.98	13.82
$4^{-+}$	11.05	10.25	10.13	10.17	10.16
$4^{+-}$		11.93	11.77	11.59	11.41
$2^{\pm+}$	7.55	6.87	6.70	6.70	6.64
$2^{\pm+*}$	9.96	9.11	8.97	9.01	8.99
$2^{\pm-}$		8.59	8.40	8.19	7.97
$2^{\pm-*}$		10.83	10.68	10.52	10.35
$1^{\pm+}$	9.95	9.19	9.05	9.07	9.05
$1^{\pm-}$		10.87	10.70	10.52	10.33
$3^{\pm+}$	8.78	8.06	7.91	7.92	7.88
$3^{\pm-}$		9.76	9.58	9.39	9.18

Table 4: Best fit spectrum of the adjoint-mixing flux tube model to the SU( $N$ ) glueball masses, in units of the string tension.

direct mixing			
group	$\alpha$	$\gamma$	$\chi_5^2/\text{d.o.f}$
SU(2)	–	$-0.42 \pm 0.12$	1.6
SU(3)	$2.17 \pm 0.6$	$0.57 \pm 0.10$	1.0
SU(4)	$2.15 \pm 0.6$	$0.41 \pm 0.10$	1.1
SU(5)	$1.98 \pm 0.6$	$0.28 \pm 0.10$	1.3
SU( $\infty$ )	$1.36 \pm 0.6$	$-.03 \pm 0.11$	.65

Table 5: Best fit parameters of the direct mixing model.

$m_G/\sqrt{\sigma}$					
state	SU(2)	SU(3)	SU(4)	SU(5)	SU( $\infty$ )
$0^{++}$	4.67	4.37	4.19	4.13	4.19
$0^{++*}$	7.84	6.98	6.84	6.84	6.22
$0^{+++}$	9.77	7.66	7.43	7.11	7.07
$0^{--}$		6.03	5.82	5.64	5.21
$0^{--*}$		8.86	8.69	8.56	8.24
$0^{---}$		10.90	10.76	10.65	10.38
$0^{-+}$	13.86	13.66	13.52	13.48	13.32
$0^{+-}$		14.43	14.25	14.15	14.01
$4^{-+}$	10.13	10.04	9.90	9.91	10.13
$4^{+-}$		11.92	11.76	11.62	11.29
$2^{\pm+}$	7.35	6.83	6.67	6.64	6.76
$2^{\pm+*}$	9.86	8.92	8.79	8.80	8.90
$2^{\pm-}$		8.58	8.39	8.22	7.84
$2^{\pm-*}$		10.83	10.68	10.54	10.24
$1^{\pm+}$	10.88	9.03	8.89	8.88	9.07
$1^{\pm-}$		10.87	10.70	10.55	10.21
$3^{\pm+}$	8.59	7.96	7.80	7.79	7.95
$3^{\pm-}$		9.76	9.58	9.42	9.06

Table 6: Best fit spectrum of the direct-mixing flux tube model to the SU( $N$ ) glueball masses, in units of the string tension.

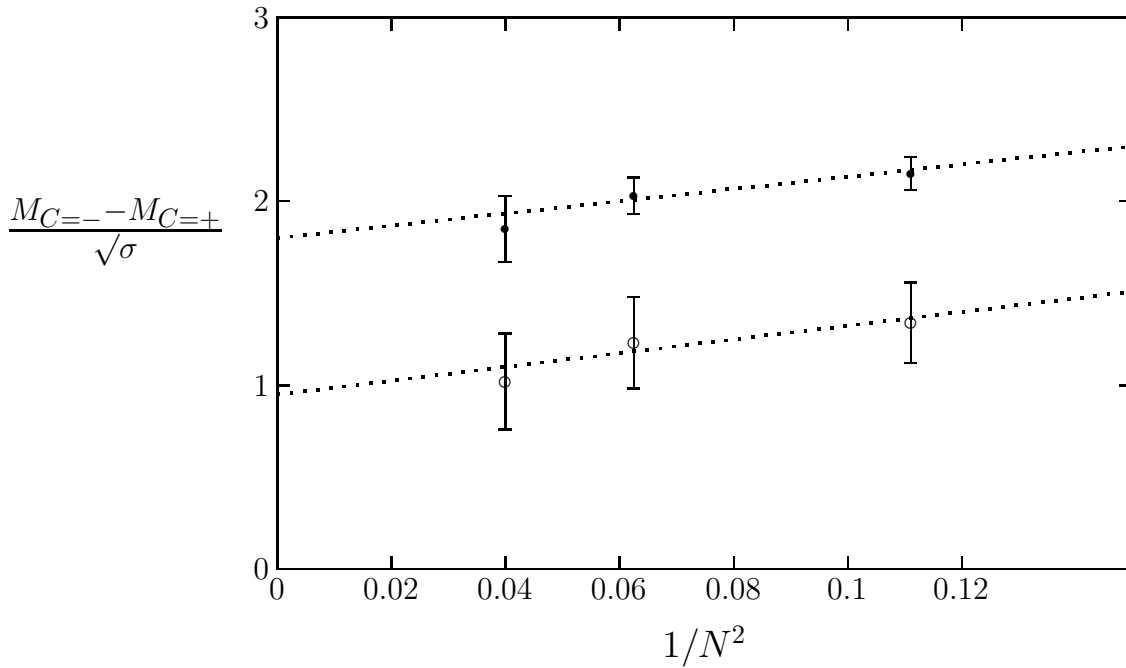


Figure 1: Some of the observed  $SU(N)$   $C = \pm$  splittings plotted versus  $1/N^2$ : the mass difference between the  $0^{--}$  and the  $0^{++}$  (●) and that between the  $2^{\pm-}$  and the  $2^{\pm+}$  (○). As  $N \rightarrow \infty$  the dependence is expected to be linear in  $1/N^2$ , i.e. like the straight lines added to the plot to guide the eye.

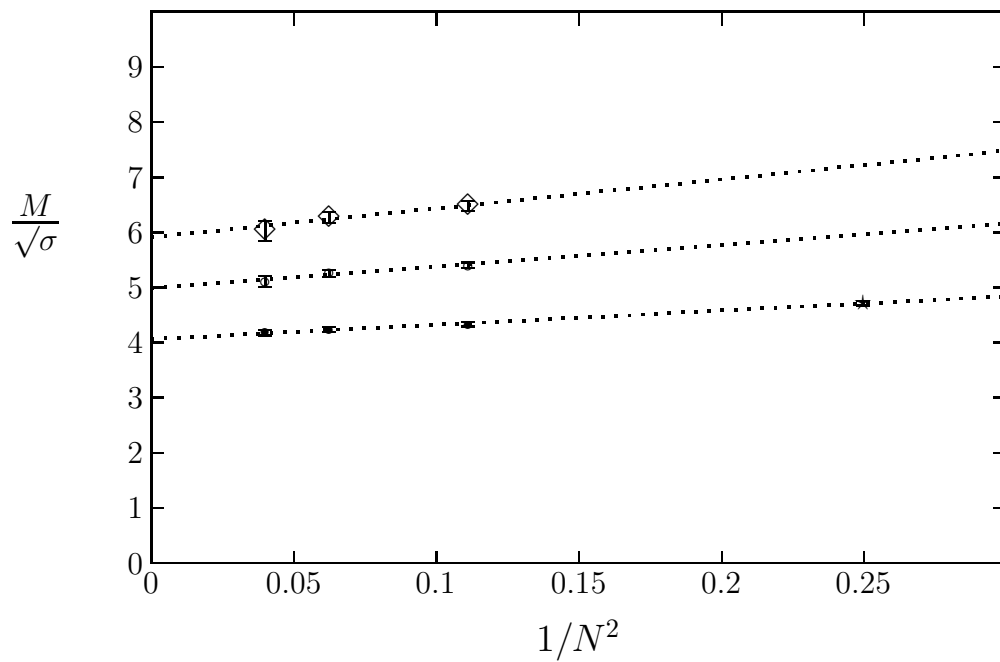


Figure 2: The SU(2)  $0^+$  mass ( $\star$ ), the SU( $N \geq 3$ )  $0^{++}$  masses ( $\bullet$ ), the SU( $N \geq 3$ )  $0^{--}$  masses ( $\diamond$ ), and the average of the  $0^{++}$  and  $0^{--}$  masses ( $\circ$ ), plotted against  $1/N^2$ ; with the expected large- $N$  linear dependence shown in each case.

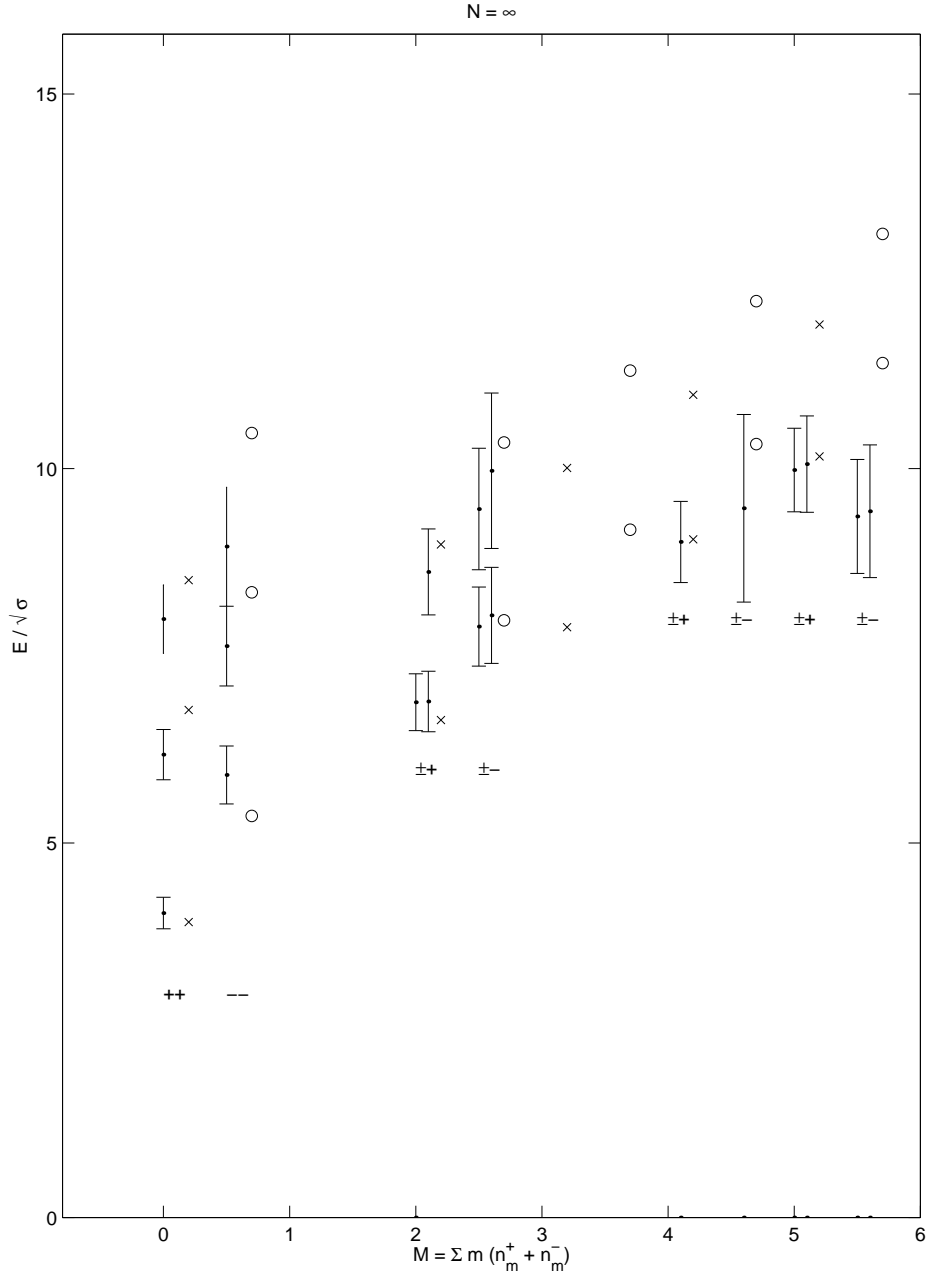


Figure 3: The spectrum for the adjoint mixing mechanism compared to lattice data at  $N = \infty$ . The x-axis gives the total phonon number  $M$ . The  $0^{-+}$  and  $0^{+-}$  are compared with  $M=4$ , and states with  $J=1$  are compared with  $M=5$ .

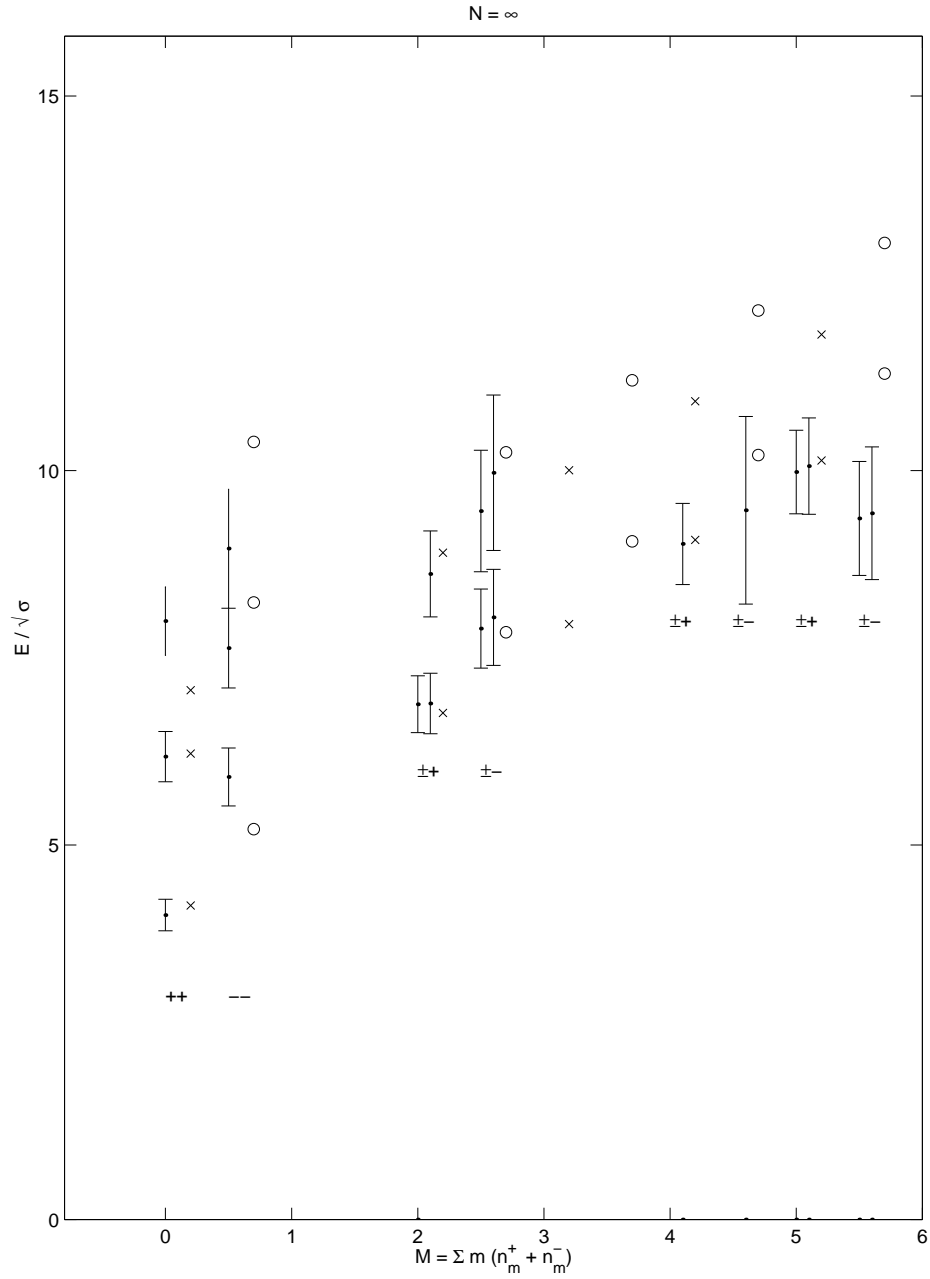


Figure 4: The spectrum for the direct mixing mechanism compared to lattice data at  $N = \infty$ . The x-axis gives the total phonon number  $M$ . The  $0^{-+}$  and  $0^{+-}$  are compared with  $M=4$ , and states with  $J=1$  are compared with  $M=5$ .